Adipocyte Long-Noncoding RNA Transcriptome Analysis of Obese Mice Identified *Lnc-Leptin*, Which Regulates Leptin

Kinyui Alice Lo,[1,2] Shiqi Huang,[3] Arcinas Camille Esther Walet,[2] Zhi-chun Zhang,[2] Melvin Khee-Shing Leow,[2,4,5,6] Meihui Liu,[3] and Lei Sun[1,2]

Diabetes 2018;67:1045–1056 | https://doi.org/10.2337/db17-0526

Obesity induces profound transcriptome changes in adipocytes, and recent evidence suggests that long-noncoding RNAs (lncRNAs) play key roles in this process. We performed a comprehensive transcriptome study by RNA sequencing in adipocytes isolated from interscapular brown, inguinal, and epididymal white adipose tissue in diet-induced obese mice. The analysis revealed a set of obesity-dysregulated lncRNAs, many of which exhibit dynamic changes in the fed versus fasted state, potentially serving as novel molecular markers of adipose energy status. Among the most prominent lncRNAs is *Lnc-leptin*, which is transcribed from an enhancer region upstream of leptin (*Lep*). Expression of *Lnc-leptin* is sensitive to insulin and closely correlates to *Lep* expression across diverse pathophysiological conditions. Functionally, induction of *Lnc-leptin* is essential for adipogenesis, and its presence is required for the maintenance of *Lep* expression in vitro and in vivo. Direct interaction was detected between DNA loci of *Lnc-leptin* and *Lep* in mature adipocytes, which diminished upon *Lnc-leptin* knockdown. Our study establishes *Lnc-leptin* as a new regulator of *Lep*.

Obesity has reached an epidemic level worldwide (1). Central to the obesity problem are adipocytes, which play a dual role of storing excess energy as triglycerides and secreting adipokines that exert systemic effects on metabolic homeostasis (2). Governing adipose tissue function is a set of expressed transcripts and proteins, many of which are dysregulated upon obesity. To discover novel obesity genes, transcriptome analysis has been extensively carried out in both mouse and human adipose tissues (3–7), but most studies primarily have focused on protein-coding genes. Long-noncoding RNAs (lncRNAs) are relatively new players in the field of gene regulation (8,9). We and others have shown that lncRNAs are essential regulators of adipogenesis, insulin sensitivity, and thermogenesis (10–12). By using RNA sequencing (RNA-Seq) on three types of mouse adipose tissues, namely inguinal white adipose tissue (iWAT), epididymal WAT (eWAT), and interscapular brown adipose tissue (BAT), followed by de novo transcriptome assembly, we have built a catalog of >1,500 mouse adipose lncRNAs (13). Another catalog of lncRNAs that regulate energy metabolism in liver, adipose tissue, and muscle has been built on the basis of microarray data (14).

Mutation in leptin (*Lep*), a circulating adipokine released from adipocytes, leads to an extreme form of obesity exemplified by *ob/ob* mice (15). A few reports of obese patients who harbor the *Lep* mutation exist, and such patients are responsive to recombinant leptin treatment (16,17). Great interest exists in understanding the regulation of the leptin gene. By using leptin-bacterial artificial chromosome (BAC) enhanced green fluorescent protein transgenic mice, a region 4.5 kilobases (kb) upstream of *Lep*, acts as an adipocyte-specific enhancer, and this region is bound by the transcription factor FOSL2 (18). A similar strategy reveals a completely different element required for *Lep* expression in vivo: a nuclear factor Y-bound element −16.5 kb upstream of the *Lep* transcription start site (19).

[1]Institute of Molecular and Cell Biology, Singapore
[2]Cardiovascular & Metabolic Disorders, Duke-NUS, Singapore
[3]Food Science and Technology Program, Department of Chemistry, National University of Singapore, Singapore
[4]Clinical Nutrition Research Centre, Singapore Institute for Clinical Sciences, Agency for Science, Technology and Research, Singapore
[5]National University Health System, Singapore
[6]Department of Endocrinology, Tan Tock Seng Hospital, Singapore

Corresponding author: Lei Sun, sun.lei@duke-nus.edu.sg.

Received 4 May 2017 and accepted 27 February 2018.

This article contains Supplementary Data online at http://diabetes.diabetesjournals.org/lookup/suppl/doi:10.2337/db17-0526/-/DC1.

To evaluate the changes of lncRNA transcriptome systemically upon obesity, we performed RNA-Seq on adipocytes isolated from BAT, iWAT, and eWAT of control and diet-induced obese mice. We identified 68 lncRNAs that are differentially expressed upon obesity, termed obesity-regulated lncRNAs in adipocytes (lnc-ORIAs). Specifically, we focused on one particular lnc-ORIA, *Lnc-leptin*, which is located in an enhancer region upstream of *Lep* and highly correlates to the expression of *Lep*. By using multiple independent loss-of-function approaches, we show that *Lnc-leptin* regulates the expression of *Lep* in vitro and in vivo.

RESEARCH DESIGN AND METHODS

Diet-Induced Obesity Models

Male mice on the C57BL/6 background were kept at the Duke-NUS animal facilities. Mice were fed normal chow diet (ND) or high-fat diet (HFD) (#D12492; Research Diets) for 16 weeks commenced upon weaning at age 3 weeks.

Primary Adipocyte Culture and Differentiation

Inguinal fat pads from 3-week-old C57BL/6 pups were excised, minced, and digested in collagenase solution at 37°C for 20 min. The suspension was filtered through 100-μm strainers and spun at 2,000 rpm for 5 min. The pelleted stromal vascular fraction (SVF) was resuspended in 10 mL DMEM supplemented with 10% newborn calf serum (Invitrogen), 100 units/mL penicillin, 100 μg/mL streptomycin, and 10 μg/mL gentamicin (Invitrogen). Cells were grown to confluence, and differentiation was initiated at day 0 with DMEM containing 10% FBS, 0.5 μmol/L dexamethasone, 850 nmol/L insulin, 0.25 mmol/L 3-isobutyl-1-methyxanthine, and 1 μmol/L rosiglitazone for 2 days. Cells were then incubated in DMEM containing 10% FBS and 170 nmol/L insulin for 2 more days. After day 4, cells were maintained for 2 more days in DMEM containing 10% FBS. Experiments were performed on mature adipocytes at day 6.

Adipocytes and SVF Isolation From Adipose Tissue

Adipose tissues were excised from mice and immediately minced in a collagenase solution comprising 0.2% collagenase (C6885; Sigma) and 2% BSA dissolved in Hanks' balanced salt solution (Gibco). Minced tissues were transferred to a 50-mL tube and incubated at 37°C for 20 min (for eWAT and iWAT) or 40 min (for BAT) at 500 rpm. Subsequently, 10 mL complete DMEM was added. Cell resuspensions were filtered through 100-μm strainers, spun at 2,000 rpm for 5 min, and washed once with PBS. The floating adipocyte layer and the pelleted SVF were collected separately. The SVF was treated with ammonium chloride solution (#07800; STEMCELL Technologies) to lyse red blood cells.

Lnc-Leptin Knockdown by Using Short Hairpin RNAs

Sequences targeting *Lnc-leptin* were cloned into a retroviral vector pSUPER (oligoengine). Short hairpin RNA (shRNA) sequences are listed in Supplementary Table 4. Retroviral vectors were transfected into packaging cell line 293T cells by using X-tremeGENE 9 (Roche). Virus-containing media were harvested 48 h posttransfection and used to infect primary preadipocytes at ~60% confluence supplemented with 8 μg/mL polybrene. Media were changed the next day, and cells were induced to differentiate 48 h postinfection.

Lnc-Leptin Knockdown by Using Dicer Substrate Small Interfering RNAs or Antisense Oligos In Vitro

For knocking down *Lnc-leptin* in preadipocytes to assess its role in adipogenesis, dicer substrate small interfering RNA (DsiRNA) or antisense oligos (ASOs) and their respective controls were transfected into day −2 preadipocytes (>90% confluence) by using lipofectamine (6 μL/mL; Life Technologies). Media were changed the next day, and cells were induced to differentiate 48 h posttransfection. For knocking down *Lnc-leptin* in primary mature adipocytes, a reverse transfection protocol was used (20). DsiRNA 200 nmol/L (Integrated DNA Technologies) or ASOs 150 nmol/L (GapmeRs; Exiqon) mixed with lipofectamine in Opti-MEM medium (6 μL/mL) were added to each well of a 24-well plate precoated with 0.1% gelatin. Mature primary adipocytes at day 6 were trypsinized and reseeded onto the oligo-lipofectamine mix. Medium was changed the next day, and knockdown efficiency was measured 48 h posttransfection. The sequences of DsiRNAs and ASOs used in this study are listed in Supplementary Tables 5 and 6, respectively.

Lnc-leptin Knockdown by Using ASOs In Vivo

Eight- to 12-week-old C57BL/6 male mice were anesthetized. Hair located at the inguinal area was removed with a trimmer, the underlying skin incised, and the inguinal adipose tissue exposed. Control ASO or ASO *Lnc-leptin* (20 mg/kg) were injected into the left- and right-side inguinal adipose tissue (~50 μL/injection), respectively. The surgical wounds were closed with sutures and disinfected with 70% ethanol. Adipose tissues from both sides of the inguinal depot were excised 48 h postinjection, and RNA was extracted and subjected to quantitative RT-PCR.

Chromatin Immunoprecipitation

Preadipocytes or mature adipocytes were trypsinized and resuspended in PBS. A two-step cross-linking protocol was used (21) as follows: Cells were incubated with 1.5 mmol/L ethylene glycol-bis (Sigma) at room temperature for 30 min followed by 1% formaldehyde for 10 min. Cross-linking was stopped by quenching with 0.125 mol/L glycine. The chromatin immunoprecipitation (ChIP) experiment was performed as previously described (22). Five micrograms MED1 antibody (A300-793A; Bethyl Laboratories) were used for immunoprecipitation, and normal rabbit IgG (sc-2027; Santa Cruz Biotechnology) was used as control. ChIP primers used in this study are listed in Supplementary Table 7.

Chromatin Conformation Capture

Chromatin conformation capture (3C) was performed as previously described (23), with modifications. Briefly, mouse adipose cells and tissues were cross-linked with 1% formaldehyde for 10 min, and the reaction was quenched by

125 mmol/L glycine for 5 min. Lysed nuclei were resuspended in 500 μL 1.2× restriction enzyme buffer before incubation at 65°C for 20 min with 22.5 μL 20% SDS followed by an additional 1 h of incubation at 37°C. Next, 150 μL 20% Triton X-100 was added, and samples were incubated at 37°C for another 1 h. Samples were then digested with 800 units XbaI (New England BioLabs) by incubating at 37°C overnight. After restriction enzyme digestion, 40 μL 20% SDS was added to the digested nuclei and incubated at 65°C for 15 min, and 6.125 mL 1.15× ligation buffer and 375 μL 20% Triton X-100 were added to dilute the total DNA to favor intramolecular ligation. The diluted sample was incubated at 37°C for 1 h before the addition of 100 units T4 DNA ligase (New England BioLabs) at 16°C for 4 h followed by 30 min at room temperature. Samples were finally decross-linked at 65°C overnight with an addition of 300 μg proteinase K (Thermo Fisher Scientific) before phenol-chloroform extraction and ethanol precipitation. Samples were further purified by QIAquick Spin columns (QIAGEN) and total DNA concentration quantified using NanoDrop. BAC that spans the whole locus of interest is RP24-369M21. All primers were designed to be within a region of 25–150 base pairs (bp) from the restriction enzyme digestion site and are unidirectional from the 5′ side of the restriction fragment. Primers were designed by using Primer3 software (Supplementary Table 8). Quantitative real-time PCR was carried out with SYBR Green Master Mix on the ABI ViiA 7. Semiquantitative PCR analysis of these primers pairs using the control template reconfirmed that there was only a single PCR product of the correct size when visualized on a 2% agarose gel. The identities of the PCR products also were confirmed through direct sequencing. To obtain data points for normalized relative interaction in the final results, cycle threshold (Ct) values of the 3C template were first normalized with values from an internal primer of control interaction frequencies, which commonly used the Ercc3 locus in mouse (23,24). Each quantitative PCR was carried out in duplicate, and 3C validations were repeated four to six times independently for each condition.

Hierarchical Clustering

Clustering was done in Cluster software and visualized in TreeView. For each model and for each gene, the gene expression value in fragments per kilobase of transcript per million (fpkm) was log-transformed and mean-centered before clustering.

Western Blot and Real-time PCR

Antibodies used for Western blot analysis were leptin (Ab16227; Abcam), Pparg (sc-7273; Santa Cruz Biotechnology), and β-actin antibody (A1978, 43 kD; Sigma) as loading control. Total RNA was extracted by using RNeasy Mini Kit (QIAGEN). Sequences of quantitative PCR primers are listed in Supplementary Table 3.

RNA-Seq Library Preparation, Sequencing, and Analysis

One microgram total RNA was used for each RNA-Seq library preparation according to the manufacturer's instructions (New England BioLabs), and sequencing was done on HiSeq 2000 (Illumina). Pair-end reads from each sample were aligned to the mouse genome (mm10 build) using TopHat version 2.0.9. Differential expression between HFD and ND samples was quantified using Cuffdiff 2.1.1. Differentially expressed genes are those that have a log-twofold change of >1 or < -1 and $q < 0.05$ compared with the control condition. We also required that the differentially expressed genes used for downstream analysis have an fpkm >1 in any of the conditions.

Gene Ontologies and Pathway Analysis

For obesity-induced protein-coding genes, gene ontology (GO) and network analysis was performed using GeneGo (Thomson Reuters). For obesity-induced lncRNAs, GO and motif analysis was done with Genomic Regions Enrichment of Annotations Tools (GREAT) software (25).

Study Approval

All studies involving animals have been approved by the institutional review board of Duke-NUS.

RESULTS

Transcriptome Analysis of Adipocytes From Three Different Adipose Depots Identified a Set of lnc-ORIAs

To evaluate the changes of adipocyte lncRNA transcriptome systemically during obesity, we isolated adipocytes from BAT, iWAT, and eWAT of mice fed an HFD or ND by using a collagenous digestion and fractionation method (Fig. 1*A*). Because adipose tissue is infiltrated with macrophages and other immune cells upon obesity (26), this step enriches for adipocytes and minimizes the contribution from the other cell types. *Lep*, an adipocyte-specific gene, was enriched >100-fold in the floating adipocyte layer compared with the pelleted SVF (Fig. 1*B*). In contrast, expression of the macrophage marker F4/80 (*Emr1*) was highly enriched in the SVF compared with adipocytes (Fig. 1*B*). Lineage marker expression, such as Hoxc9, Hoxc10, and Ucp1, both before and after collagenous digestion indicated that the BAT and isolated adipocytes were not contaminated by one another (Supplementary Fig. 1).

We performed RNA-Seq on adipocytes isolated from three different adipose depots (BAT, iWAT, and eWAT) in HFD and ND. More than 200 million paired-end reads in total were aligned (Supplementary Table 1) to Ensembl protein-coding genes (mm10) and a published adipose lncRNA catalog (13). To assess whether obesity affects global mRNA and lncRNA transcriptomes in a similar manner, we performed unsupervised hierarchical clustering on the sets of expressed mRNAs and lncRNAs (fpkm >1), respectively. The main branch of the dendrogram, with the exception of BAT that only has one data set per condition, primarily separates all samples on the basis of diet rather than sites of origin in both mRNA and lncRNA clustering (Fig. 1*C*). There are 353 protein-coding genes differentially expressed in adipocytes from the three different depots upon obesity (Fig. 1*D*), including *Lep* (15), *Sfrp5* (27), and

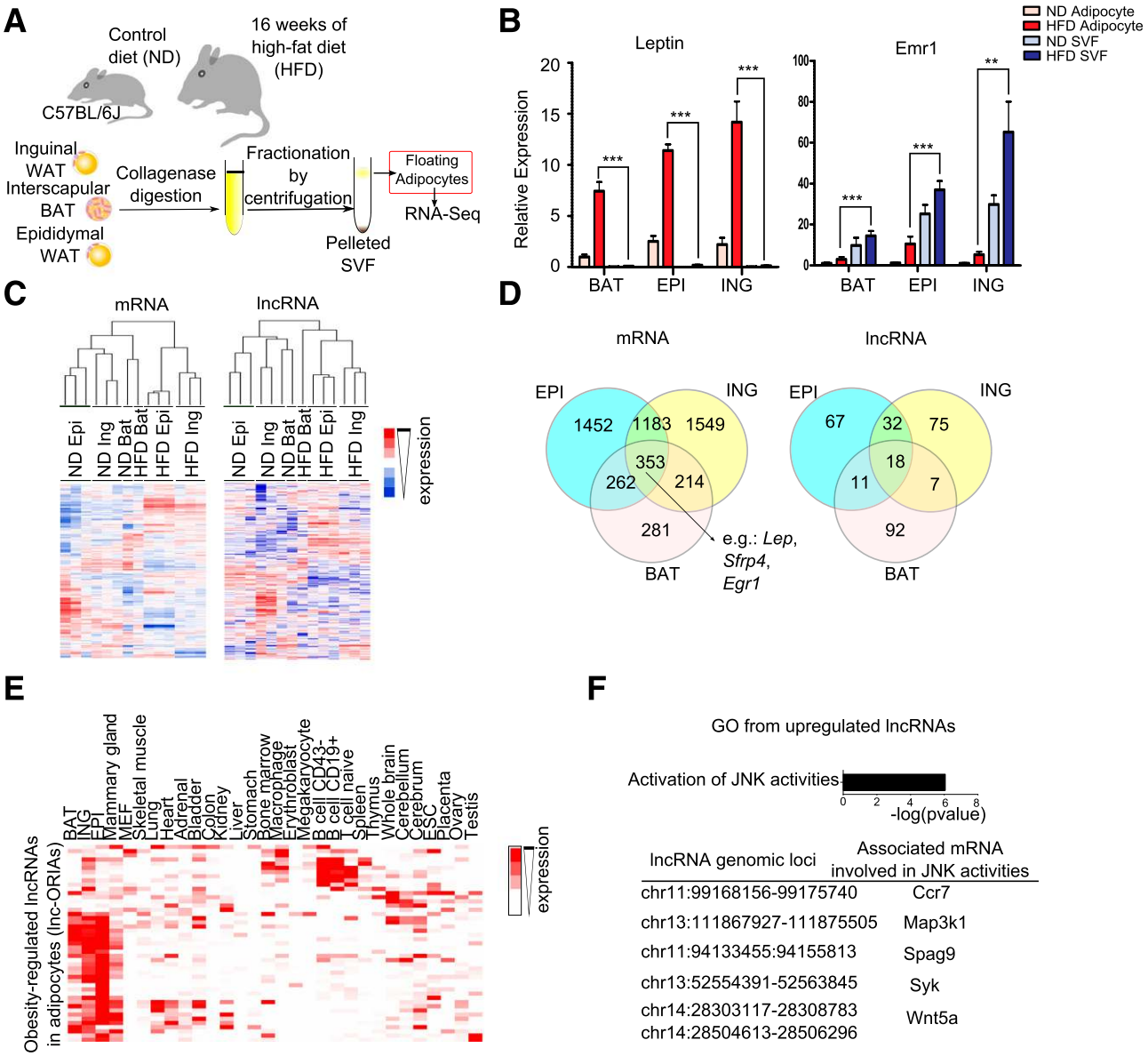

Figure 1—Adipocyte lncRNA transcriptomes reveal meaningful insights of diet-induced obesity. *A*: Study schematic: C57BL/6J male mice were fed an ND or HFD for 16 weeks after weaning at age 3 weeks. Adipocytes were isolated from interscapular BAT, iWAT (ING), and eWAT (EPI) by collagenase digestion and centrifugation. RNA was extracted from the floating adipocyte layer and subjected to high-throughput RNA-Seq. *B*: Quantitative PCR analysis of an adipocyte-specific gene (*Lep*) and a macrophage marker (*Emr1*) on isolated adipocytes and pelleted SVF. For both genes, the expression in the various adipose tissues or fractions was normalized to that in BAT adipocyte, which has a value of 1. Adipocyte and SVF were compared in the HFD condition (n = 4–6). Expression differences of adipocyte and SVF for ND-fed mice also were significant (data not shown). Data are mean ± SEM. $^{**}P < 0.01$, $^{***}P < 0.001$ compared with the control condition by two-tailed Student t test. *C*: Unsupervised hierarchical clustering of fpkm from expressed (fpkm >1 in all conditions) mRNAs (n = 9,640) and lncRNAs (n = 355) from adipocytes of mice fed ND vs. HFD. The height of each arm of the dendrogram above the heat maps represents the distance between the different data sets. Normalized gene expression data (fpkm values after log-transformation and mean centering) are shown. *D*: Venn diagram showing overlap of obesity-regulated mRNAs (left) and lncRNAs (right) among adipocytes from BAT, ING, and EPI. *E*: Relative abundance of the identified obesity-induced lncRNAs across 30 different mouse tissues using RNA-Seq data from ENCODE (Encyclopedia of DNA Elements). BAT, ING, and EPI are shown in the first three columns. *F*: GO analysis of the obesity-induced lncRNAs using GREAT software. The lncRNA-mRNA pairs that are associated with the GO term activation of JNK activities are shown. chr, chromosome; ESC, embryonic stem cell; MEF, mouse embryonic fibroblast.

Egr1 (28), many of which have previously been identified and studied in the context of obesity. Network analysis of the obesity-upregulated genes using GeneGo, which incorporates curated data from published literature, identified the nuclear factor-κB subunits *RelA*, *Esr1*, and *Creb1* to be the top three transcription factor hubs (Supplementary Fig. 2*A*) to mediate the expression changes. GO analysis identified developmental processes ($P < 1E-17$), response to stress ($P < 9E-14$), and cell differentiation ($P < 3E-11$) as the top categories associated with the obesity-upregulated protein-coding genes (Supplementary Fig. 2*B*). These processes, together with the transcription factors nuclear factor-κB,

Esr1, and *Creb1*, have been implicated in previous studies (29,30), indicating that the current data do reflect biological changes of adipocytes during obesity.

Compared with protein-coding genes, less is known about adipocyte lncRNA changes upon obesity. The data indicate that 68 lncRNAs are significantly differentially expressed between ND and HFD in at least two of the three types of adipocytes we profiled (Fig. 1*D*). We termed them lnc-ORIAs (Supplementary Table 2). Many lnc-ORIAs display adipocyte-specific expression (Fig. 1*E* and Supplementary Fig. 3). By using GREAT, which infers function of genomic regions on the basis of the ontology annotations of their neighboring protein-coding genes (25), we found that activation of c-Jun N-terminal kinase (JNK) activity is the only significant ($P <$ 1E-6) GO category associated with the obesity-induced lncRNAs (Fig. 1*F*). Furthermore, the C/EBPβ motif was found to be enriched from this group of induced lncRNA genes (Supplementary Fig. 1*C*). JNK has been shown to play a central role in obesity (31), whereas C/EBPβ has been implicated in adipose insulin resistance (32). Together, the current data suggest that meaningful biological insight could be gleaned from transcriptome analysis of lncRNAs and that lncRNAs could be important regulators of obesity.

Many lnc-ORIAs Are Regulated in Various Metabolic Conditions and Bound by PPARG

To confirm the expression changes of the lnc-ORIAs identified from the high-throughput RNA-Seq, we isolated RNA from independent cohorts of ND- and HFD-fed mice, and we confirmed the expression changes of 10 selected lnc-ORIAs on the basis of their expression values, fold changes, and gene structures (Fig. 2*A*). Of the 10 lnc-ORIAs chosen on the basis of their higher expression level and unambiguous gene structure, 9 were induced upon obesity and 1 was repressed (*lnc-ORIA1*). The expression changes generally occurred in all three tissues profiled, although tissue-specific differences exist (e.g., *lnc-ORIA6*). To test whether the changes of these lncRNAs are a general feature in other obesity models, we examined their expression in adipose tissue from *ob/ob* and control mice and found that the expression of all 10 lnc-ORIAs changes in the same direction as that in diet-induced obesity, with 8 reaching significance (Supplementary Fig. 4).

To investigate whether these selected lnc-ORIAs are responsive to alteration of nutritional status, we measured their expression in adipose tissue of ad libitum mice (fed) and mice that underwent an overnight fast (fasted). Nine of 10 of these targets (except *lnc-ORIA7*) had significantly decreased expression in the various adipose tissues upon fasting (Fig. 2*B*). Fasting and diet-induced obesity represent two extremes of the nutritional spectrum, one being an acute nutrient-deprived state and the other a chronic nutrient-excess state. The majority of the lncRNAs examined displayed an inverse correlation pattern of expression in these two conditions (Fig. 2*C*), suggesting that these lnc-ORIAs could be molecular sensors reflecting the energy status in adipose tissue.

Previous studies have shown that tissue- or condition-specific lncRNAs, similar to protein-coding genes, often are bound and regulated by key transcription factors. By using published PPARG ChIP sequencing data from mouse WAT and BAT (33), we found that one-half of the 10 lnc-ORIAs studied are bound by PPARG at their promoters (3 are shown in Fig. 2*D*), suggesting that many of these lnc-ORIAs are transcriptionally regulated by PPARG in vivo.

Lnc-Leptin Is an Enhancer lncRNA

We are particularly intrigued by *lnc-ORIA9* (hereafter *Lnc-leptin*), which lies 28 kb upstream of *Lep*, a satiety hormone secreted by adipocytes that acts centrally to regulate systemic metabolism and immunity (17). *Lnc-leptin* has two exons, and it overlaps largely with an uncharacterized known transcript *Gm30838*, which shares the same splice sites as *Lnc-leptin* (Fig. 3*A*). The promoter of *Lnc-leptin* has an open chromatin conformation as shown by published DNase sequencing data. There is positive H3K4 trimethylation (H3K4Me3) signal and RNA polymerase II binding at the transcription start site of *Lnc-leptin* as shown by published ChIP sequencing data (Fig. 3*B* and Supplementary Fig. 5*A*), indicating that this gene is actively transcribed in adipose tissue. *Lnc-leptin* also harbors positive H3K4 methylation 1 (H3K4Me1) and H3K27 acetylation (H3K27Ac) markers in WAT (Fig. 3*B*); these histone modifications typically associate with enhancers (H3K4Me1) and active enhancers (H3K27Ac) (34). Similar histone mod-ification architecture in this region also was observed in BAT (Supplementary Fig. 5*B*). Furthermore, to test whether the *Lnc-leptin* region is associated with MED1, a component of the mediator complex known to bridge enhancer regions with the general transcription machinery and RNA polymerase II at gene promoters (35), we performed a ChIP exper-iment in differentiated white primary adipocyte culture (Fig. 3*C*). Because *Lnc-leptin* is undetectable in brown adi-pocyte culture, the ChIP experiment was only performed in differentiated white primary adipocytes. The ChIP results indicate that MED1 is recruited to the promoter regions of *Lnc-leptin* and *Lep* (Fig. 3*C*). Taken together, *Lnc-leptin* is transcribed from an enhancer near *Lep* and is an enhancer lncRNA.

Expression of *Lnc-Leptin* Is Highly Correlated to That of *Lep*

We next investigated the spatial and temporal expression of *Lnc-leptin*. By using mouse SVF-derived primary adipocyte culture, we found that expression of *Lnc-leptin* increases gradually as differentiation progresses in a similar manner as *Lep* and *Pparg* (Fig. 4*A*). To assess whether the expression of *Lnc-leptin* is specific to adipose tissue, we measured its expression in 20 different mouse tissues and found that it is highest in eWAT followed by iWAT and BAT. *Lnc-leptin* also is expressed, albeit at a much lower level, in testicle and eye (Fig. 4*B*). Of note, the tissue-specific expression of *Lnc-leptin* highly mirrors that of *Lep* (Fig. 4*B*). To examine whether the expression of these two genes are correlated, we plotted the expression of *Lnc-leptin* and *Lep* across a variety of conditions, including HFD versus ND (n = 45), *ob/ob* versus wild-type (n = 9), and fasted versus fed (n = 42) mouse

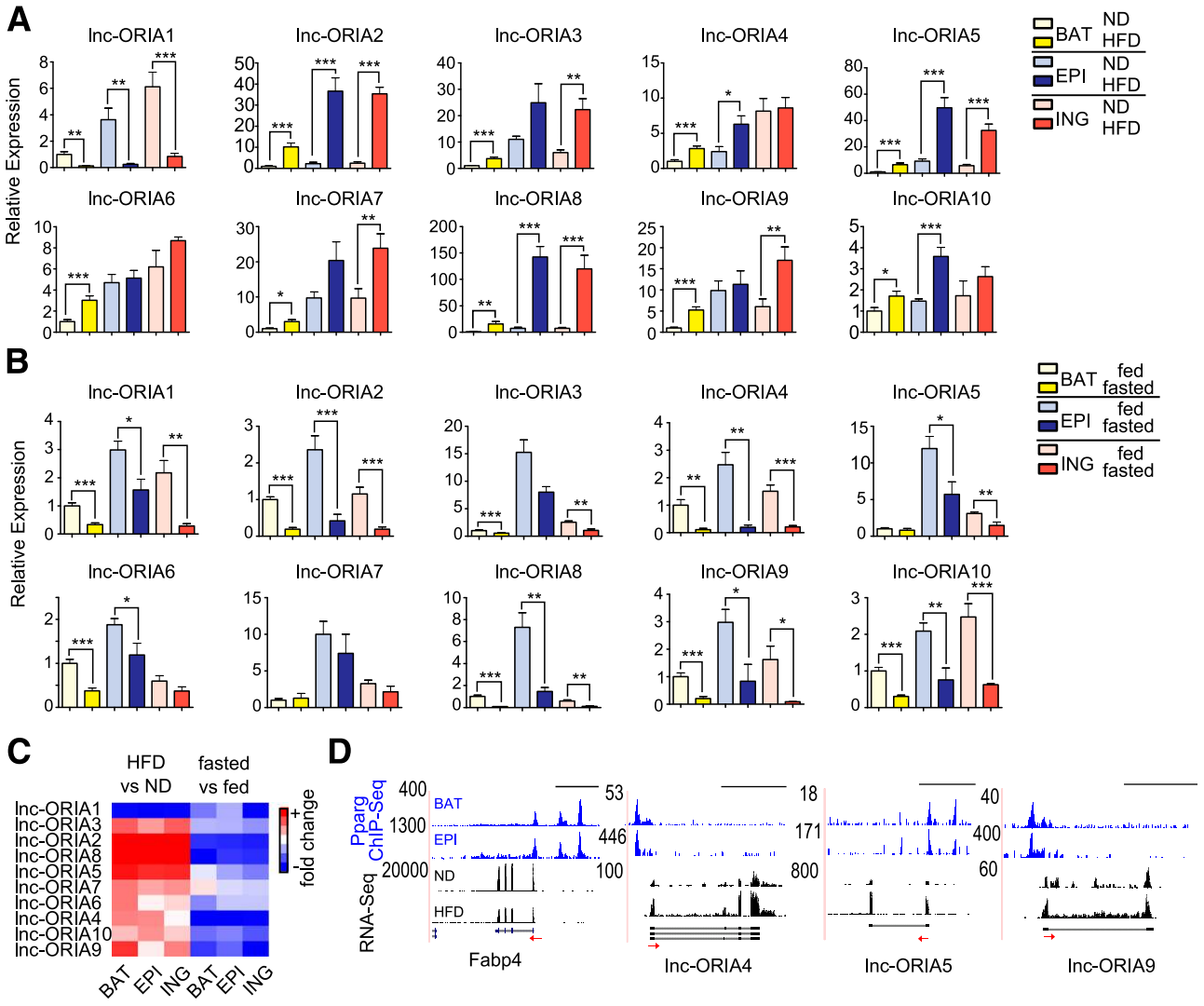

Figure 2—Selected lnc-ORIAs are dynamically regulated in diverse pathophysiological conditions. *A*: Quantitative PCR analysis of selected lnc-ORIAs from BAT, iWAT (ING), and eWAT (EPI) of mice fed ND ($n = 8$) vs. HFD ($n = 7$). *B*: Quantitative PCR analysis of selected lnc-ORIAs from BAT, ING, and EPI of mice fasted overnight ($n = 6$) vs. fed control ($n = 7$). For *A* and *B*, data are mean ± SEM. $^*P < 0.05$, $^{**}P < 0.01$, $^{***}P < 0.001$ compared with control by two-tailed Student *t* test. *C*: Heat map illustrating the expression fold changes of the 10 selected lnc-ORIAs under HFD vs. ND and fasted vs. fed conditions. Red represents an increase in expression in HFD (or fasted) vs. ND (or fed), and blue represents a decrease in expression in HFD (or fasted) vs. ND (or fed). *D*: University of California, Santa Cruz, genome browser tracks showing that promoters of *Fabp4* and selected lnc-ORIAs are bound by PPARG in mouse BAT and EPI. The RNA-Seq tracks were generated in the current study and correspond to the expression changes upon HFD in EPI, whereas the PPARG ChIP-Seq data were from published data (GSE43763) (33). Arrows indicate the direction of transcription. Scale bars = 5 kb.

adipose tissues. A tight correlation ($r > 0.76$) was found between the expression of *Lnc-leptin* and *Lep* in all examined conditions (Fig. 4*C*). To also assess whether *Lnc-leptin* and *Lep* respond similarly to hormonal signaling, we treated differentiated primary adipocytes with various agents known to alter the expression of *Lep*. Acute insulin stimulation induced *Lep* expression (36,37); we found that such an increase was accompanied by an induction of *Lnc-leptin* (Fig. 4*D*). Conversely, upon tumor necrosis factor-α (TNF-α) and norepinephrine treatment where *Lep* was repressed (38,39), *Lnc-leptin* expression was concomitantly reduced (Fig. 4*E* and *F*). Taken together, we have demonstrated a close correlation between the expression of *Lnc-leptin* and *Lep*, pointing to a potential causative relationship between them.

Lnc-Leptin Is Required for Adipogenesis

To investigate the role of *Lnc-leptin* during adipogenesis, we used two independent strategies to knock it down in primary adipocyte cultures: shRNAs and DsiRNAs. First, we infected primary white preadipocytes with retrovirus-harboring control shRNA or shRNA constructs targeting *Lnc-leptin*. Cells then were differentiated per normal, and RNA was harvested at day 6 postdifferentiation. *Lnc-leptin* knockdown using two different shRNA constructs led to a >80% reduction of the gene (Fig. 5*A*). Furthermore, it almost completely blocked

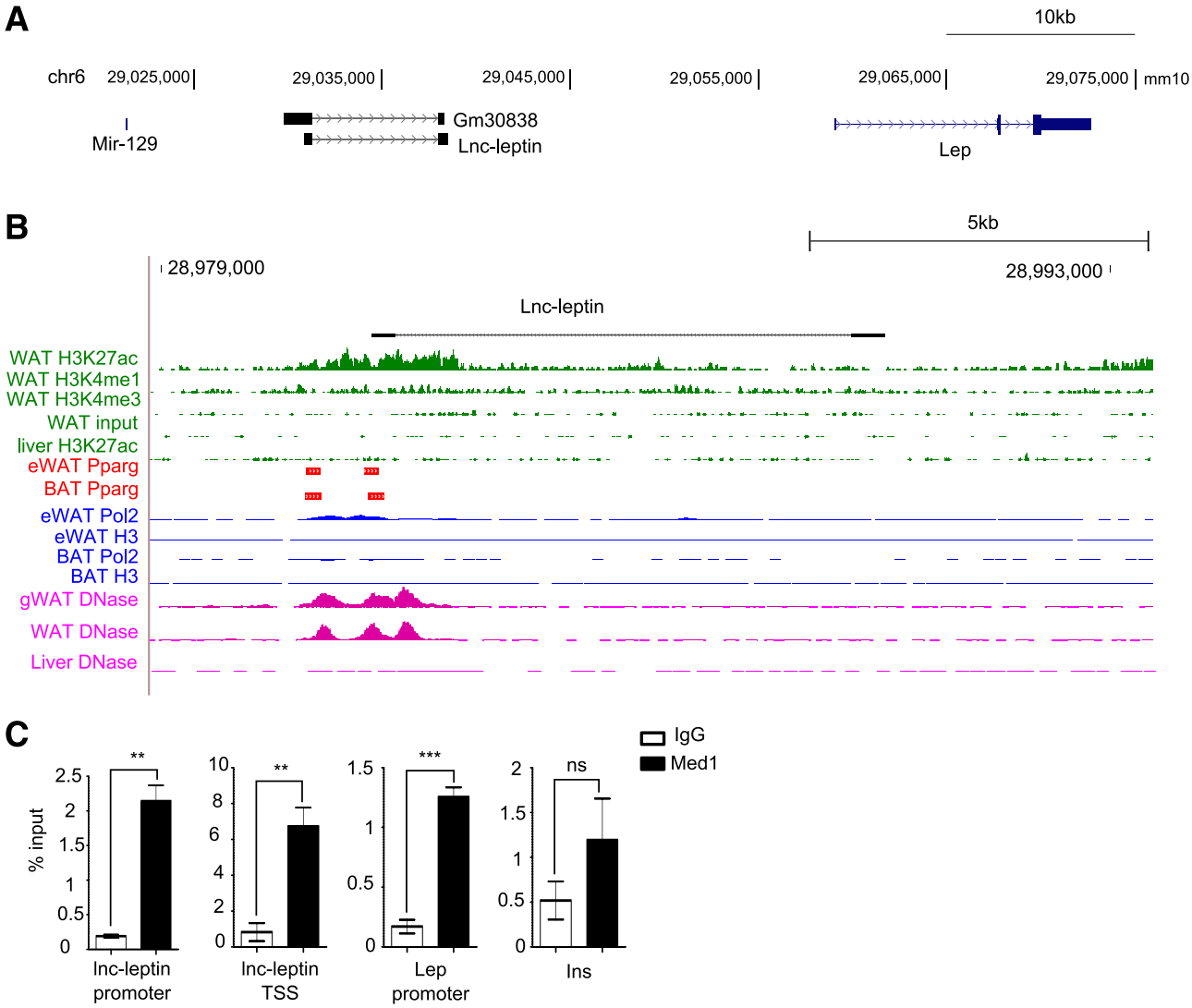

Figure 3—The identification of *Lnc-leptin*, an enhancer lncRNA upstream of *Lep*. *A*: Genomic location of *Lnc-leptin* in mm10. Both *Lnc-leptin* and *Lep* are on the positive strand and 28 kb apart. *B*: Mouse DNaseI hypersensitivity, histone modification, RNA polymerase II (Pol2) binding profile, and Pparg-bound sites in a 15-kb region around *Lnc-leptin*. DNaseI hypersensitivity profile of genital fat pad (gWAT), fat pad (WAT), and liver from 8-week-old mice (pink) is from ENCODE (Encyclopedia of DNA Elements)/University of Washington. Histone modification data (H3K4Me3, H3K4Me1, and H3K27Ac) of pooled WAT from eWAT and iWAT (green) is from GSE92590. eWAT and BAT RNA Pol2 and H3 control ChIP sequencing data (blue) are from GSE63964. PPARG ChIP sequencing data from eWAT and BAT (red) is from GSE43763. *C*: ChIP experiment using MED1 antibody showing MED1 binding in the promoters of *Lnc-leptin* and *Lep* in white mature primary adipocytes differentiated in vitro (day 7) at *Lnc-leptin* promoter, *Lnc-leptin* transcription start site (TSS), and *Lep* promoter. Insulin genomic region (Ins) is used as negative control. Data are mean ± SEM ($n = 3$). $^{**}P < 0.01$, $^{***}P < 0.001$ compared with the control condition by two-tailed Student *t* test. chr, chromosome; ns, not significant.

adipocyte differentiation. Oil Red O staining showed very little lipid accumulation in the knockdown cells compared with the control (Fig. 5*B*). This defect was accompanied by a reduction in *Lep* and the adipocyte-markers *Pparg* and *Adipoq* (Fig. 5*C*). Similar results were obtained when *Lnc-leptin* was knocked down in preadipocytes by DsiRNA (Fig. 5*D*), suggesting that *Lnc-leptin* is required for adipogenesis.

Lnc-Leptin Regulates the Expression of *Lep* in Mature Adipocytes

Depletion of *Lnc-leptin* during adipogenesis results in severe inhibition of cell differentiation that can indirectly block *Lep* expression, so whether *Lnc-leptin* can directly affect *Lep* expression is unclear. To test this question, we knocked down *Lnc-leptin* in mature adipocytes. Primary white preadipocytes differentiated into mature adipocytes, and DsiRNAs or ASOs were transfected into the cells by using a reverse transfection protocol (20). Both methods resulted in a >80% reduction in *Lnc-leptin* expression (Fig. 5*E* and *F*), and both were accompanied by a concomitant reduction of *Lep* expression. Of note, the expression of two mature adipocyte markers, *Pparg* and *Adipoq*, was also significantly reduced upon *Lnc-leptin* knockdown, but the extent of reduction was less. To test whether knocking down *Lnc-leptin* would affect *Lep*

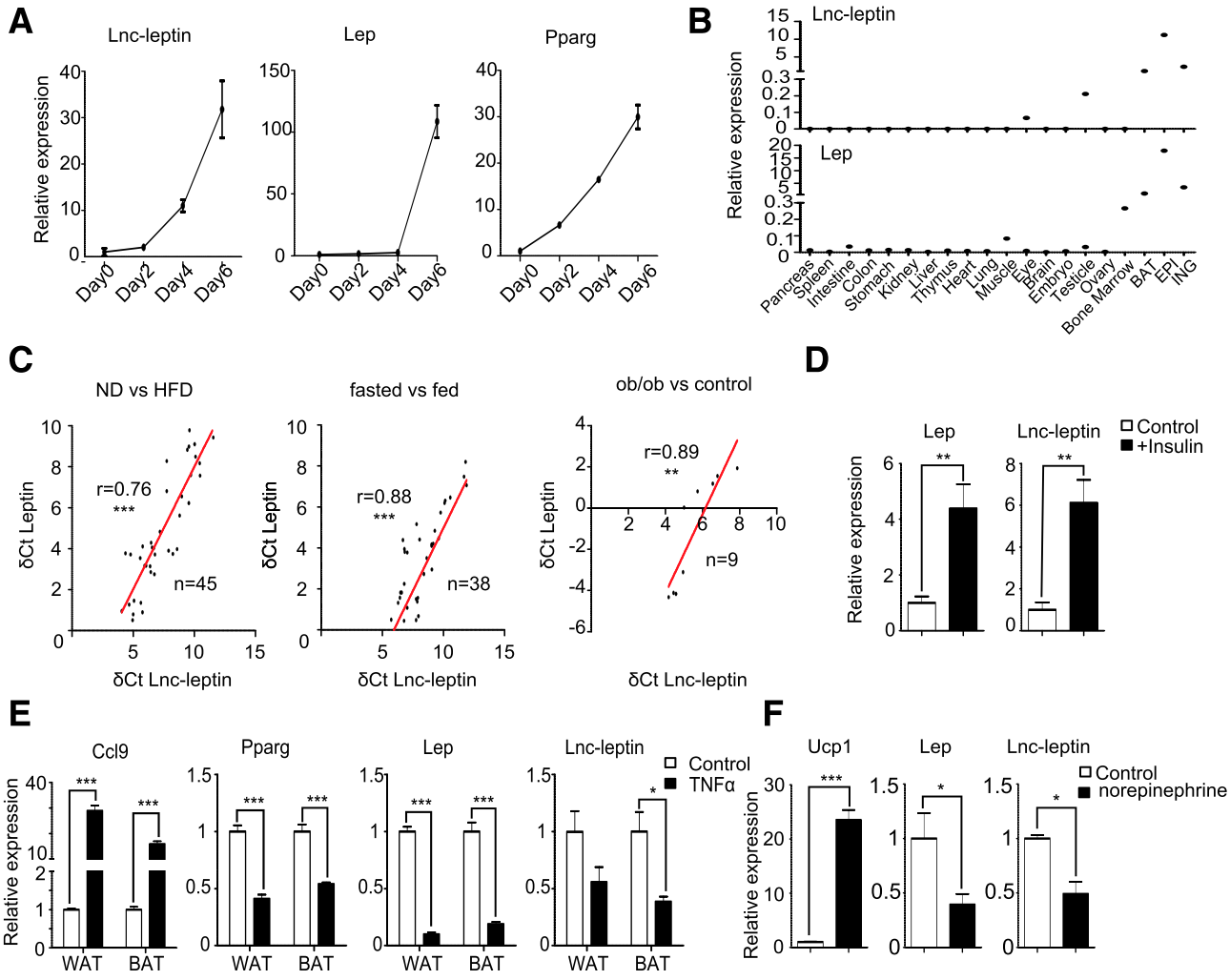

Figure 4—Expression of *Lnc-leptin* is highly correlated to that of *Lep*. *A*: Quantitative PCR analysis of expression of *Lnc-leptin*, *Lep*, and *Pparg* upon differentiation of primary white adipocytes ($n = 4$). Gene expression was expressed relative to day 0. *B*: *Lnc-leptin* and *Lep* RNA expression measured by quantitative PCR in 20 different mouse tissues. *C*: Correlation between the expression of *Lnc-leptin* and *Lep* under various conditions in mouse adipose tissue: ND vs. HFD ($n = 45$), fasted vs. fed ($n = 38$), and *ob/ob* vs. control ($n = 9$). δCt of *Lnc-leptin* (Ct of *Lnc-leptin* – Ct of housekeeping gene *Rpl23*) were plot against δCT of *Lep*. *D*: Mature primary white adipocytes (day 6) were treated with 100 nmol/L insulin for 3 h ($n = 4$). Gene expression was expressed relative to control treatment. *E*: Mature primary brown and white adipocytes were treated with 2.5 nmol/L TNF-α for 24 h ($n = 4$). Gene expression was expressed relative to control treatment. *F*: Mature primary white adipocytes were treated with 1 μmol/L norepinephrine for 24 h ($n = 4$). For *D*–*F*, quantitative PCR results were calculated using *Rpl23* as the housekeeping gene. Data are mean ± SEM. $^*P < 0.05$, $^{**}P < 0.01$, $^{***}P < 0.001$ compared with the control model by two-tailed Student *t* test. EPI, eWAT; ING, iWAT.

expression in vivo, we injected ASO against *Lnc-leptin* directly into one side of mouse inguinal tissue, with the contralateral side injected with a scrambled control. Tissues were harvested 2 days later for expression analysis. Both *Lnc-leptin* and *Lep* expression were significantly reduced upon ASO injection (Fig. 5*G*), and the decrease was accompanied by a less significant reduction in *Lep* and *Pparg* mRNA (Fig. 5*G*). *Lnc-leptin* knockdown also led to a decrease in LEP but not PPARG protein expression (Fig. 5*H*), arguing that the reduction of LEP protein is not due to a decreased PPARG protein level. Taken together, knocking down *Lnc-leptin* affects *Lep* expression in mature adipocytes both in vitro and in vivo.

To test whether *Lnc-leptin* is sufficient to promote *Lep* expression, we used retroviral vector to overexpress *Lnc-leptin* in primary white adipocyte culture. Overexpression of *Lnc-leptin* did not promote the expression of *Lep* or other adipocyte markers (Supplementary Fig. 6). Thus, *Lnc-leptin* is necessary but not sufficient to promote *Lep* expression or adipogenesis.

Lnc-Leptin Mediates a Loop Formation Between Genomic Loci of *Lep* and *Lnc-Leptin*

The above studies demonstrate that *Lnc-leptin* is transcribed from an enhancer region and positively regulates the expression of *Lep*. A common mechanism many enhancers use is to form a long-distance interaction with the promoter of their target genes to facilitate transcription by recruiting positive regulators. We hypothesize that *Lnc-leptin* is involved in such an interaction near the *Lep* promoter. To test

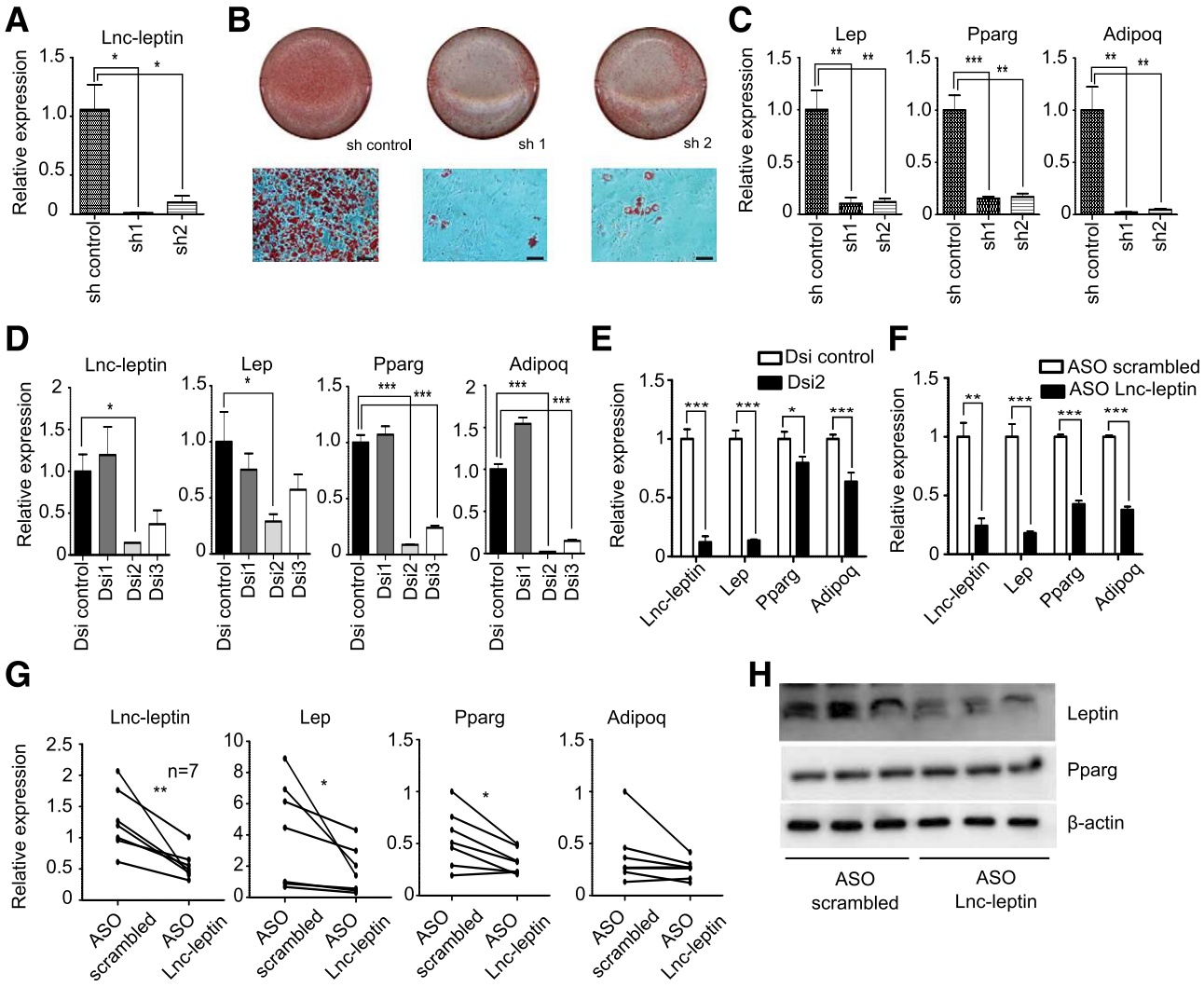

Figure 5—Knocking down *Lnc-leptin* represses *Lep*. *A*: Retrovirus-mediated transduction of primary preadipocytes (day −2) using control and two separate shRNAs targeting *Lnc-leptin*. Cells were induced to differentiate, and RNA was harvested at day 6. Expression of *Lnc-leptin* at day 6 was measured by quantitative PCR (n = 4). *B*: Oil Red O staining showing adipocyte differentiation defect upon *Lnc-leptin* knockdown by shRNAs. Scale bar = 100 μm. *C*: Expression of three adipocyte marker genes at day 6 upon shRNA transduction as described in *A* (n = 4). *D*: Transfection of DsiRNA control or DsiRNAs targeting *Lnc-leptin* (Dsi1, Dsi2, and Dsi3) was performed at the preadipocyte stage at day −2, and RNA was extracted at day 4. Expression of *Lnc-leptin* and other adipocyte marker genes were measured at day 4 using quantitative PCR (n = 4). *E*: Expression of *Lnc-leptin* and other adipocyte markers in mature primary adipocytes reverse transfected with DsiRNA control or a specific DsiRNA targeting *Lnc-leptin* (Dsi2). Transfection was performed at day 6, and RNA was extracted 48 h later (n = 4). *F*: Expression of *Lnc-leptin* and other adipocyte markers in mature primary adipocytes reverse transfected with ASO targeting *Lnc-leptin* or scrambled control. Transfection was performed at day 6, and RNA was extracted 48 h later (n = 4). *G*: *Lnc-leptin* was knocked downed in vivo in mouse iWAT using ASO *Lnc-leptin* and compared with scrambled control (n = 7). For each mouse, ASO *Lnc-leptin* was injected on one side and scrambled control on the contralateral side. Tissue was harvested, and RNA was extracted 48 h postinjection. *H*: Western blots showing the reduced protein expression of *Lep* in mouse iWAT after knockdown of *Lnc-leptin* using ASO. $^*P < 0.05$, $^{**}P < 0.01$, $^{***}P < 0.001$ compared with the control model by two-tailed Student t test.

long-range chromatin interaction between the genomic loci of *Lnc-leptin* and *Lep*, 3C experiments were performed to interrogate the chromatin structure around these two genes (Fig. 6*A*). By using the promoter of *Lep* as an anchoring point, the genomic locus that encompasses exon2 of *Lnc-leptin* was found to interact with *Lep* promoter (Fig. 6*B*). The 3C-ligated fragment was sequenced to confirm that it is indeed a hybrid product ligated from the two separate genomic regions. This interaction was attenuated upon knocking down *Lnc-leptin* (Fig. 6*C*), indicating that *Lnc-leptin* is required for the looping event. We propose that *Lnc-leptin* is a novel enhancer lncRNA that regulates *Lep* expression by bringing *Lep* with its upstream enhancer and the transcriptional machinery to proximity (Fig. 6*D*).

DISCUSSION

Whole-genome sequencing efforts in the past two decades have revolutionized our understanding of the mammalian genome; now recognized is that the mammalian genome is pervasively transcribed to generate thousands of noncoding RNA species, including lncRNAs (40). Several lncRNAs play

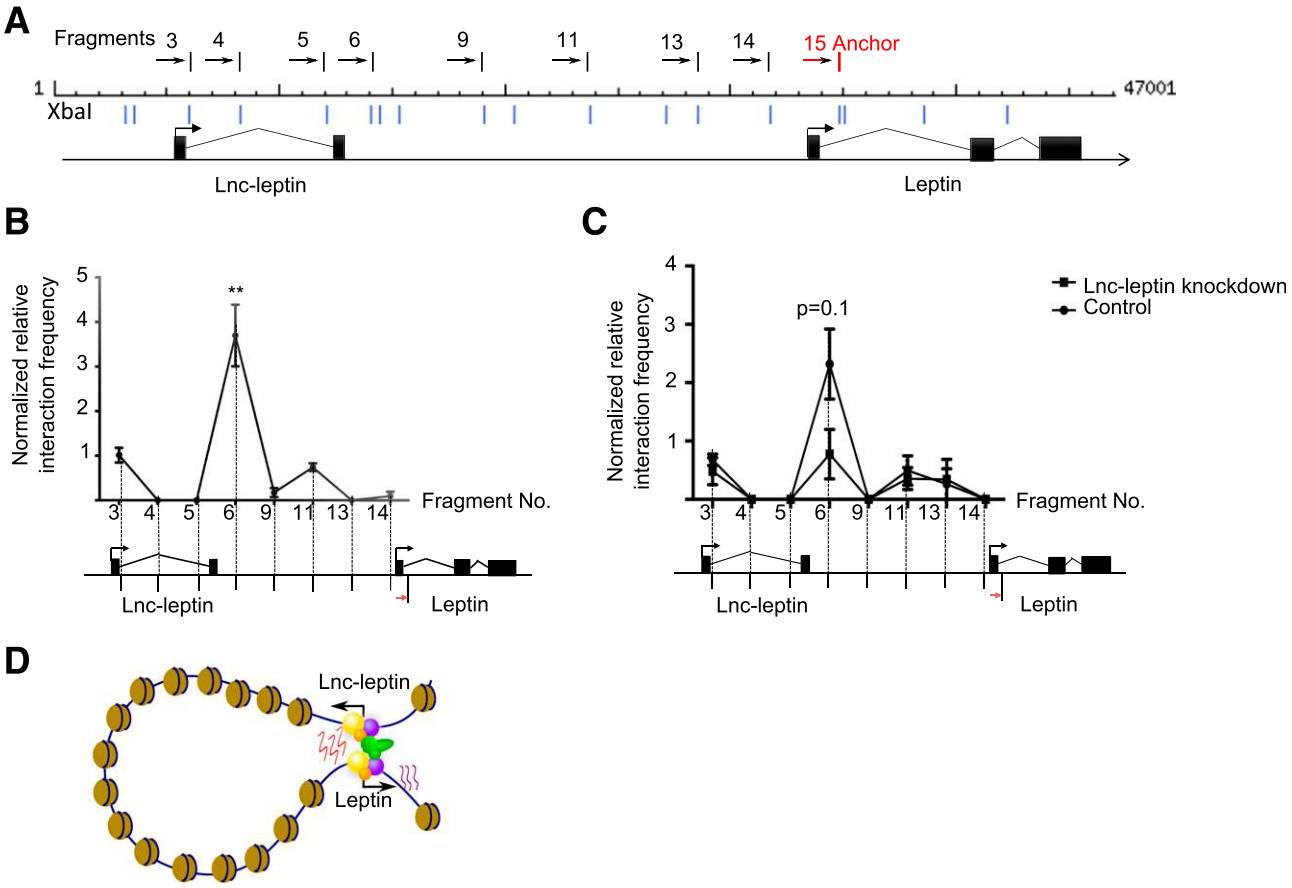

Figure 6—Chromatin looping between *Lnc-leptin* and *Lep* is diminished upon *Lnc-leptin* knockdown in mature adipocytes. *A*: A 3C experiment was performed to explore the three-dimensional chromosome configuration in the proximity of *Lnc-leptin* and *Lep*. Blue lines indicate sites at which restriction enzyme XbaI cuts into a 47,000-bp genomic region spanning *Lnc-leptin* and *Lep*. Arrows next to the XbaI cut sites indicate the direction of primers used in the 3C experiment. The anchor primer (anchoring fragment 15) encompasses the transcription start site of *Lep*. Rectangles indicate the exons of *Lnc-leptin* and *Lep* genes, whereas linking lines represent introns. *B*: Interaction frequency between the anchoring point and upstream distal fragments was determined by quantitative PCR ($n = 4$) and normalized to BAC and control regions in primary adipocytes. Chromatin looping was detected between fragment 6 (which contains exon 2 of *Lnc-leptin*) and anchoring fragment 15. *C*: The 3C-quantitative PCR result of mouse primary adipocytes with *Lnc-leptin* knockdown against its scrambled control using ASO. A noticeable decrease is seen in interaction frequency between anchoring fragment 15 and fragment 6 upon *Lnc-leptin* knockdown ($P = 0.1$). *D*: Model of how *Lnc-leptin* potentially regulates *Lep* expression: *Lnc-leptin* is required for chromatin interaction between the genomic loci of *Lnc-leptin* and *Lep*. Expression of *Lnc-leptin* enhances the expression of *Lep* by bringing together the two genes and their transcription machinery. $^{**}P < 0.01$ compared with control by two-tailed Student *t* test.

key roles in regulating energy metabolism (41). We systemically profiled lncRNAs in three types of adipocytes in diet-induced obese mice and identified 68 regulated lncRNAs, termed lnc-ORIAs. Among the lnc-ORIAs, we focused on *Lnc-leptin* because of its proximity to *Lep*. The local genomic structure and histone modification patterns of *Lnc-leptin* are reminiscent of those of a typical enhancer. However, in contrast to the neuronal enhancer RNAs, which generally are unspliced and lack polyadenylated tails (42), *Lnc-leptin* was identified through polymerase A tail-enriched RNA-Seq and consists of two exons. *Lnc-leptin* also differs from the bidirectional enhancer-derived transcripts (43) because our directional RNA-Seq did not detect any transcript coming from the opposite direction (Fig. 2*D*).

Knockdown experiments using DsiRNA and ASO indicated that knocking down *Lnc-leptin* leads to a concomitant reduction in *Lep* expression both in vitro and in vivo (Fig. 5), suggesting that the RNA transcript itself rather than the act of transcription confers the function of the lncRNA. *Lnc-Leptin* positively regulates the expression of *Lep*, similar to those lncRNAs that activate the expression of their neighboring protein-coding genes (44–46). We showed by 3C experiment that *Lnc-leptin* is likely to be required for chromatin interaction between exon 2 of *Lnc-leptin* and the promoter of *Lep* (Fig. 6). This putative interaction brings the two genes in proximity in a three-dimensional space that potentially enhances the expression of *Lep* (Fig. 6). In our proposed model (Fig. 6*D*), the *Lnc-leptin* transcript acts as a bridge to enhance the interaction between the *Lep* promoter and enhancer: It could directly interact with *Lep* promoter or merely serve as a scaffold to bring transcription factors and histone-modifying proteins together. We acknowledge that many details about the mechanism remain unanswered. For example, we do not know what proteins *Lnc-leptin* directly

interacts with, whether *Lnc-leptin* forms an RNA-DNA duplex directly with the enhancer or the promoter (or both), or whether *Lnc-leptin* can interact with other DNA segments. These questions warrant further investigation in future studies.

The regulatory mechanism of *Lnc-leptin* on *Lep* may not account for its effects on adipogenesis. Knockdown of *Lnc-leptin* during adipogenesis resulted in a severe reduction of lipid accumulation and expression of mature adipocytes markers (Fig. 5*A–D*). Because the formation of mature adipocytes in *ob/ob* mice is not impaired, we believe that *Lnc-leptin* may use an LEP-independent mechanism to regulate adipogenesis, which warrants further investigation. In mature adipocytes, knocking down *Lnc-leptin* seems to reduce the expression of adipocyte markers *Pparg* and *Adipoq* in addition to *Lep*. How such a reduction occurs remains to be answered.

In two previous studies, the genomic region of *Lnc-leptin* was not identified as a cis-regulatory element that regulates the adipose-specific expression of *Lep*. Both studies used BAC transgenic reporter mice to identify the cis- and transregulatory elements of *Lep* in vivo. Wrann et al. (18) identified that a region containing the three *Lep* exons, both introns, and 5.2 kb of the 5′ flanking sequence was sufficient to drive adipocyte-specific enhancer green fluorescent protein expression, whereas Lu et al. (19) identified −22 to 8.8 kb of *Lep* as the region required for adipose-specific *Lep* expression. Both studies excluded the genomic location of *Lnc-leptin*, which lies ∼28 kb upstream of *Lep*. It is plausible that *Lnc-leptin* is not primarily involved in the basal expression of *Lep* but instead serves as a metabolic sensor to regulate the expression of *Lep* upon various energy statuses in adipocytes. For a dynamically regulated gene like *Lep*, its regulation is likely to be controlled by the coordination of multiple regulatory mechanisms. The current study reveals a new layer of regulatory complexity, whereas earlier studies (18,19) have identified several cis- and transregulatory factors. These layers of regulation are not mutually exclusive but are all orchestrated by the cellular energy status. Together, they weave a sophisticated network to rapidly adjust *Lep* expression to respond to nutritional level alteration.

Funding. This research was supported by the National Medical Research Council (NMRC) under its Cooperative Basic Research Grant (CRBG) (NMRC/CBRG/0070/2014 and NMRC/CBRG/0101/2016) and Open Fund-Individual Research Grant (OFIRG) (NMRC/OFIRG/0062/2017) and by the Ministry of Education–Singapore Tier 2 grant MOE2017-T2-2-015. This work was supported by the RNA Biology Center at Cancer Science Institute Singapore, Duke-NUS, from funding by the Ministry of Education's Tier 3 grant MOE2014-T3-1-006. S.H. and M.L. are supported by an NMRC-CBRG New Investigator Grant (NMRC/BNIG/2027/2015). This work was supported by National Research Foundation Singapore fellowship NRF-2011NRF-NRFF 001-025 and the Tanoto Initiative in Diabetes Research to L.S.

Duality of Interest. No potential conflicts of interest relevant to this article were reported.

Author Contributions. K.A.L., S.H., A.C.E.W., Z.-c.Z., M.K.-S.L., and M.L., performed the experiments and analyzed the data. K.A.L. and L.S. designed the project, interpreted the data, and wrote the manuscript. L.S. is the guarantor of this work and, as such, had full access to all the data in the study and takes responsibility for the integrity of the data and the accuracy of the data analysis.

References

1. Haslam DW, James WP. Obesity. Lancet 2005;366:1197–1209
2. Rosen ED, Spiegelman BM. What we talk about when we talk about fat. Cell 2014;156:20–44
3. Morton NM, Nelson YB, Michailidou Z, et al. A stratified transcriptomics analysis of polygenic fat and lean mouse adipose tissues identifies novel candidate obesity genes. PLoS One 2011;6:e23944
4. Tam CS, Heilbronn LK, Henegar C, et al. An early inflammatory gene profile in visceral adipose tissue in children. Int J Pediatr Obes 2011;6:e360–e363
5. Rodríguez-Acebes S, Palacios N, Botella-Carretero JI, et al. Gene expression profiling of subcutaneous adipose tissue in morbid obesity using a focused microarray: distinct expression of cell-cycle- and differentiation-related genes. BMC Med Genomics 2010;3:61
6. Grove KL, Fried SK, Greenberg AS, Xiao XQ, Clegg DJ. A microarray analysis of sexual dimorphism of adipose tissues in high-fat-diet-induced obese mice. Int J Obes 2010;34:989–1000
7. Kogelman LJA, Cirera S, Zhernakova DV, Fredholm M, Franke L, Kadarmideen HN. Identification of co-expression gene networks, regulatory genes and pathways for obesity based on adipose tissue RNA sequencing in a porcine model. BMC Med Genomics 2014;7:57
8. Rinn JL, Chang HY. Genome regulation by long noncoding RNAs. Annu Rev Biochem 2012;81:145–166
9. Fatica A, Bozzoni I. Long non-coding RNAs: new players in cell differentiation and development. Nat Rev Genet 2014;15:7–21
10. Sun L, Goff LA, Trapnell C, et al. Long noncoding RNAs regulate adipogenesis. Proc Natl Acad Sci U S A 2013;110:3387–3392
11. Zhao X-Y, Li S, Wang G-X, Yu Q, Lin JD. A long noncoding RNA transcriptional regulatory circuit drives thermogenic adipocyte differentiation. Mol Cell 2014;55:372–382
12. Xu B, Gerin I, Miao H, et al. Multiple roles for the non-coding RNA SRA in regulation of adipogenesis and insulin sensitivity. PLoS One 2010;5:e14199
13. Alvarez-Dominguez JR, Bai Z, Xu D, et al. De novo reconstruction of adipose tissue transcriptomes reveals novel long non-coding RNAs regulators of brown adipocyte development [published correction appears in Cell Metab 2015;21:918]. Cell Metab 2015;21:764–776
14. Yang L, Li P, Yang W, et al. Integrative transcriptome analyses of metabolic responses in mice define pivotal LncRNA metabolic regulators. Cell Metab 2016;24:627–639
15. Zhang Y, Proenca R, Maffei M, Barone M, Leopold L, Friedman JM. Positional cloning of the mouse obese gene and its human homologue [published correction appears in Nature 1995;374:479]. Nature 1994;372:425–432
16. Wabitsch M, Funcke JB, Lennerz B, et al. Biologically inactive leptin and early-onset extreme obesity. N Engl J Med 2015;372:48–54
17. Friedman J. 20 years of leptin: leptin at 20: an overview. J Endocrinol 2014;223:T1–T8
18. Wrann CD, Eguchi J, Bozec A, et al. FOSL2 promotes leptin gene expression in human and mouse adipocytes. J Clin Invest 2012;122:1010–1021
19. Lu YH, Dallner OS, Birsoy K, Fayzikhodjaeva G, Friedman JM. Nuclear factor-Y is an adipogenic factor that regulates leptin gene expression. Mol Metab 2015;4:392–405
20. Isidor MS, Winther S, Basse AL, et al. An siRNA-based method for efficient silencing of gene expression in mature brown adipocytes. Adipocyte 2015;5:175–185.
21. Zeng PY, Vakoc CR, Chen ZC, Blobel GA, Berger SL. In vivo dual cross-linking for identification of indirect DNA-associated proteins by chromatin immunoprecipitation. Biotechniques 2006;41:694, 696, 698
22. Lo KA, Bauchmann MK, Baumann AP, et al. Genome-wide profiling of H3K56 acetylation and transcription factor binding sites in human adipocytes. PLoS One 2011;6:e19778
23. Hagège H, Klous P, Braem C, et al. Quantitative analysis of chromosome conformation capture assays (3C-qPCR). Nat Protoc 2007;2:1722–1733
24. Medvedovic J, Ebert A, Tagoh H, et al. Flexible long-range loops in the VH gene region of the Igh locus facilitate the generation of a diverse antibody repertoire. Immunity 2013;39:229–244

25. McLean CY, Bristor D, Hiller M, et al. GREAT improves functional interpretation of cis-regulatory regions. Nat Biotechnol 2010;28:495–501
26. Weisberg SP, McCann D, Desai M, Rosenbaum M, Leibel RL, Ferrante AW Jr. Obesity is associated with macrophage accumulation in adipose tissue. J Clin Invest 2003;112:1796–1808
27. Mori H, Prestwich TC, Reid MA, et al. Secreted frizzled-related protein 5 suppresses adipocyte mitochondrial metabolism through WNT inhibition. J Clin Invest 2012;122:2405–2416
28. Yu X, Shen N, Zhang ML, et al. Egr-1 decreases adipocyte insulin sensitivity by tilting PI3K/Akt and MAPK signal balance in mice. EMBO J 2011;30:3754–3765
29. Manrique C, Lastra G, Habibi J, Mugerfeld I, Garro M, Sowers JR. Loss of estrogen receptor α signaling leads to insulin resistance and obesity in young and adult female mice. Cardiorenal Med 2012;2:200–210
30. Qi L, Saberi M, Zmuda E, et al. Adipocyte CREB promotes insulin resistance in obesity. Cell Metab 2009;9:277–286
31. Hirosumi J, Tuncman G, Chang L, et al. A central role for JNK in obesity and insulin resistance. Nature 2002;420:333–336
32. Lo KA, Labadorf A, Kennedy NJ, et al. Analysis of in vitro insulin-resistance models and their physiological relevance to in vivo diet-induced adipose insulin resistance. Cell Rep 2013;5:259–270
33. Rajakumari S, Wu J, Ishibashi J, et al. EBF2 determines and maintains brown adipocyte identity. Cell Metab 2013;17:562–574
34. Creyghton MP, Cheng AW, Welstead GG, et al. Histone H3K27ac separates active from poised enhancers and predicts developmental state. Proc Natl Acad Sci U S A 2010;107:21931–21936
35. Allen BL, Taatjes DJ. The mediator complex: a central integrator of transcription. Nat Rev Mol Cell Biol 2015;16:155–166
36. Buyse M, Viengchareun S, Bado A, Lombès M. Insulin and glucocorticoids differentially regulate leptin transcription and secretion in brown adipocytes. FASEB J 2001;15:1357–1366
37. Lee KN, Jeong IC, Lee SJ, Oh SH, Cho MY. Regulation of leptin gene expression by insulin and growth hormone in mouse adipocytes. Exp Mol Med 2001; 33:234–239
38. Gettys TW, Harkness PJ, Watson PM. The beta 3-adrenergic receptor inhibits insulin-stimulated leptin secretion from isolated rat adipocytes. Endocrinology 1996; 137:4054–4057
39. Ruan H, Hacohen N, Golub TR, Van Parijs L, Lodish HF. Tumor necrosis factor-alpha suppresses adipocyte-specific genes and activates expression of preadipocyte genes in 3T3-L1 adipocytes: nuclear factor-kappaB activation by TNF-alpha is obligatory. Diabetes 2002;51:1319–1336
40. Birney E, Stamatoyannopoulos JA, Dutta A, et al.; ENCODE Project Consortium; NISC Comparative Sequencing Program; Baylor College of Medicine Human Genome Sequencing Center; Washington University Genome Sequencing Center; Broad Institute; Children's Hospital Oakland Research Institute. Identification and analysis of functional elements in 1% of the human genome by the ENCODE pilot project. Nature 2007;447:799–816
41. Kornfeld J-W, Brüning JC. Regulation of metabolism by long, non-coding RNAs. Front Genet 2014;5:57
42. Kim T-K, Hemberg M, Gray JM, et al. Widespread transcription at neuronal activity-regulated enhancers. Nature 2010;465:182–187
43. Andersson R, Gebhard C, Miguel-Escalada I, et al. An atlas of active enhancers across human cell types and tissues. Nature 2014;507:455–461
44. Ørom UA, Derrien T, Beringer M, et al. Long noncoding RNAs with enhancer-like function in human cells. Cell 2010;143:46–58
45. Trimarchi T, Bilal E, Ntziachristos P, et al. Genome-wide mapping and characterization of Notch-regulated long noncoding RNAs in acute leukemia. Cell 2014; 158:593–606
46. Hsieh C-L, Fei T, Chen Y, et al. Enhancer RNAs participate in androgen receptor-driven looping that selectively enhances gene activation. Proc Natl Acad Sci U S A 2014;111:7319–7324